Thiol-Functionalized Poly(ω-pentadecalactone) Telechelics for Semicrystalline Polymer Networks

Neil Simpson,[†] Mohamad Takwa,[‡] Karl Hult,[‡] Mats Johansson,[†] Mats Martinelle,[‡] and Eva Malmström*,[†]

KTH Fibre and Polymer Technology, School of Chemical Science and Engineering, Royal Institute of Technology, Teknikringen 56-58, SE-100 44 Stockholm, Sweden, and Department of Biochemistry, School of Biotechnology, Royal Institute of Technology, AlbaNova University Center, SE-106 91 Stockholm, Sweden

Received October 31, 2007; Revised Manuscript Received February 25, 2008

ABSTRACT: Semicrystalline macromonomers based on poly(pentadecalactone), PPDL, have been synthesized by the lipase-catalyzed ring-opening of the otherwise chemically inert pentadecalactone monomer. The macromonomers were designed to have reactive thiols as end groups by the appropriate choice of initiator and chain terminator. The thiol functional macromonomers were then used together with ene monomers to give cross-linked thin films after irradiation in the molten state by UV light in the presence of a photoinitiator (Irgacure 651). Two different ene monomers were used, i.e., a tetrafunctional norbornene species and a trifunctional allyl ether maleate species, and resulted in semicrystalline cured films when cured with PPDL. An amorphous, commercially available, trifunctional thiol, trimethylolpropane tri(3-mercaptopropionate), TRIS, was also used for network formation in order to better understand the effect of crystallinity. All thiol−ene systems were found to be readily photopolymerised to high conversion. The PPDL-based networks were semicrystalline in the cross-linked state where the degree of crystallinity was found to depend on the nature of the cross-linker. Networks based on TRIS were found to be amorphous.

Introduction

Thiol−ene polymerization is a simple, versatile process for preparing polymer networks, using combinations of multifunctional alkenes and thiols.[1,2] Owing to the advantages of thiol−ene chemistry such as ease of polymerization, preparation, resistance to oxygen inhibition, solventless processing, and rapid curing, thiol−ene chemistry has found applications in areas such as dentistry,[3] microelectromechanical systems,[4] surface grafting,[5] film patterning,[6] thermoplastics,[7] and degradable biomaterials.[8] Thiol−ene chemistry has, due to the advantages discussed above, attracted a rapidly growing interest during the past 10−15 years. However, the access to thiol compounds is very limited, and their synthesis is considered to be nasty, mainly due to the formation of smelly byproduct.

Recently, we reported the simple, one pot synthesis of poly(pentadecalactone) (PPDL) using *Candida antarctica* with tailored end groups and to high conversion.[9] To synthesize a dithiol-functionalized PPDL macromonomer, the polymer chain is first initiated with 6-mercapto-1-hexanol to give 97% incorporation of the first thiol group. The enzyme then propagates the ring-opening of PDL until the monomer is consumed, whereupon γ-thiobutyrolactone is added to terminate the process by the addition of the second thiol group (with 92% incorporation). This process is simple to perform and negates many of the difficulties encountered by conventional polymer modification using thiols that include protection and deprotection steps and purification.

So far, little has been published regarding the PPDL aside from its enzymatic synthesis[10−12] and more recently for copolymer synthesis.[13−15] We were interested in PPDL since it is a hydrophobic, semicrystalline polymer with properties similar to those of low-density PE,[16] which has never been incorporated into a network and may confer PE-like properties. In addition, although crystalline polymers are more difficult to biodegrade than their amorphous analogues,[17] the ester functionality of PPDL helps to make them biodegradable,[10,18] which could give them an advantage over PE-based films.

However, the main aim of the present work is to demonstrate and evaluate the use of semicrystalline macromonomers for thermosetting and thin films applications. The inclusion of crystallinity in polymer materials can bestow a number of desirable benefits such as oxidative and chemical resistance,[19] improved strength,[20] reduced gas permeability,[20] and decreased creep. Semicrystalline monomers are also of particular interest since they can be used in powder coating formulations.[24]

Research on cross-linked, semicrystalline networks appears in a wide range of areas involving PE, liquid crystalline polymer networks,[21,22] and also in powder coating resins. Poly(ε-caprolactone), a shorter chain semicrystalline polymer than PPDL readily available by metal-assisted ring-opening polymerization, has been cross-linked using γ-radiation,[23] used to impart crystallinity to polymers as a grafted additive,[24,25] and has been used to cast thin (non-cross-linked) films.[26] Crystalline polymers have also been used to create blends of interpenetrating networks[27−29] or cross-linked using ionizing radiation.[30]

To examine the properties of thiol-functional PPDL ($PPDL_{SH}$, **3**, Figure 1) as a macromonomer for thiol−ene chemistry, we synthesized two alkene monomers: first, a tetrafunctional norbornene cross-linker (NTMP, **1**, Figure 1) and, second, a trifunctional cross-linker based upon trimethylolpropane diallyl ether maleate (TMPDEA, **2**, Figure 1). The two monomers were selected for their low volatility and different chemical nature, different degrees of functionality, and steric arrangements. They were also expected to have different rates of polymerization since norbornene is reported to react faster than most "enes" in thiol−ene chemistry.[2] To summarize, we have examined the reactivity of PPDL, a semicrystalline, low T_g (−27 °C)[16] polyester with low volatility, capped with thiol end groups for film formation with "ene" monomers (Figure 1) and analyzed the resultant network properties. The trimethylolpropane tris(2-

* Corresponding author. E-mail: mave@polymer.kth.se.
[†] School of Chemical Science and Engineering.
[‡] School of Biotechnology.

10.1021/ma702419m CCC: $40.75
Published on Web 04/25/2008

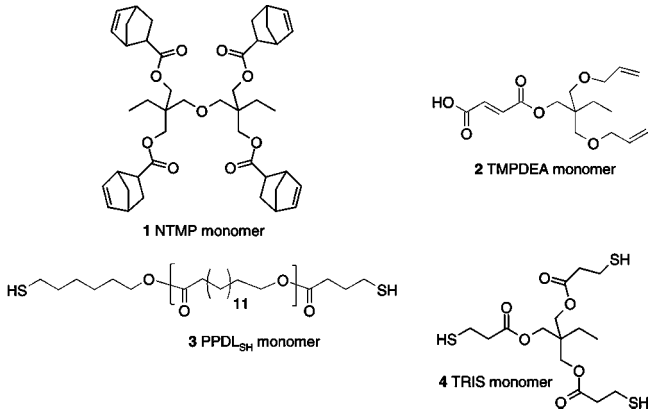

Figure 1. Monomers used for thiol−ene network formation.

mercaptoacetate) (TRIS) monomer (**4**, Figure 1) was chosen to make amorphous analogues to the crystalline networks, since it is known to work efficiently in thiol−ene chemistry. TRIS is readily available from commercial sources.

Results and Discussion

Synthesis of Monomers. The norbornene monomer (NTMP **1**, Figure 1) was synthesized via the anhydride of 5-norbornene-2-carboxylic acid in high yields. The anhydride was obtained through the DCC-mediated coupling of 5-norbornene-2-carboxylic acid, which proceeded in high yields. The reaction was monitored by ^{13}C NMR spectroscopy by the disappearance of carbonyl signals at 181 and 182 ppm and emergence of new signals at 170 and 171 ppm. The anhydride was then purified by precipitation into cold heptane from DCM to remove the remaining byproduct, *N*-acylurea. The anhydride was produced as a mix of isomers (70% endo and 30% exo, calculated by comparing the integrals of the separate isomer alkene protons in the ^{1}H NMR spectrum). The anhydride was thereafter coupled to ditrimethylolpropane (diTMP) in good yield (91%) to give the four-functional norbornene-containing monomer, NTMP, **1** (Figure 1). Upon successful esterification, the diTMP was found to consist of an average of 75% *endo* and 25% e*xo* norbornene side arms as determined by ^{1}H NMR. The methylene protons adjacent to the hydroxyl groups of diTMP (H_8) shifted downfield from 3.3 to 3.9 ppm once reacted, and the associated carbon shifted from 61.9 to 63.7 ppm accordingly. The new carbonyl signals from the ester of **1** (both isomers) can be seen to shift to downfield from the anhydride carbonyl signals at 170 and 171 ppm to the products signals at 174 and 175 ppm. The HMQC proton assignments (Figure 2) have been conducted according to HH-COSY analysis of a reported esters of 5-norbornene-2-carboxylic acid[31] and that of the unreacted reagents such as diTMP. When used with the HMQC correlation, we could identify the signals in the complex carbon spectra (that result from the isomeric mixture) and confirmed that the new carbon signal at 63.7 ppm (C_9), correlating to the protons H_8, is the methylene group next to the new norbornene ester on diTMP. In addition, the successful esterification was evidenced by the appearance of the ester stretch by FTIR at 1731 cm^{-1}. The molecular weight was determined by MALDI-TOF to 753 Da, which agrees well with the theoretical molecular weight.

The TMPDE acid monomer, TMPDEA, **2** (Figure 1), was synthesized via the acid-catalyzed ring-opening of maleic anhydride onto trimethylolpropane diallyl ether which was conducted at 80 °C in the presence of a radical inhibitor, hydroquinone, in order to avoid premature cure. The crude product was purified by medium-pressure liquid chromatography eluting with a gradient of heptane/ethyl acetate and 1% of acetic acid. The purified product was isolated as a transparent yellowish oil in 63% yield. The ^{1}H NMR spectrum indicates that alkene bond in the product is *trans* due to the quartet at 6.4 ppm, although the *cis* form can be collected from the column as a smaller fraction of the final product.

The PPDL$_{SH}$ macromonomer, **3** (Figure 1), was synthesized and analyzed according to the procedures published previously.[9] M_n was determined by SEC analysis and found to be 1500 g mol^{-1} and the PDI 2.3. MALDI-TOF was found to give a predominant signal at 1400 g mol^{-1}. However, the MALDI-TOF result is not considered to be fully reliable due to the broad molecular weight distribution in the sample.

Wet Film Formation and Curing. We studied four thiol−ene mixtures. First PPDL$_{SH}$, **3**, was reacted with NTMP, **1**, and TMPDEA, **2**. Second, TRIS, **4**, was reacted with **1** and **2** again. These combinations served two purposes: first, to examine the difference between a semicrystalline network and an amorphous network and, second, to examine the different network properties based upon monomer functionality (and reactivity). All combinations were prepared so as to have equimolar amounts of ene and thiol groups. TMPDEA comprises two allyl ether groups and one additional double bond in the maleic residue; consequently, each TMPDEA has three reactive ene groups.

In terms of the PPDL$_{SH}$, **3**, films had to be processed as a melt at 100 °C since **3** is a semicrystalline solid at room temperature. Therefore, the monomers (**1** or **2**) were mixed with PPDL$_{SH}$ as an equimolar ratio of ene to thiol end groups, to ensure all groups could theoretically react with each other. The photoinitiator (Irgacure 651, 1% w/w) and a surfactant (Texanol, 0.5% w/w) were then added, and the mixture left to melt for 15 min at 100 °C. The addition of the surfactant was required to reduce the surface tension of the glass substrates, so that a more uniform film could be obtained regardless of the monomer composition used. Substrates were also tried without surfactant, such as polished steel, Teflon, and glass, but all gave an orange peel film, irrespective of which monomer was used with PPDL$_{SH}$. Once the film was cast, it was immediately cured in the molten state by UV radiation (500 mJ/cm^2) and then left to cool and recrystallize. The films became opaque after cooling and were transformed from a waxy brittle material before curing to a solid, flexible film after curing. NTMP has to be treated with care, as premature, thermally initiated, polymerization can take place if left too long at too high a temperature. The TRIS-based amorphous networks were prepared in the same manner, except for the heat treatment; to give transparent films, surfactant was required to prevent an orange peel effect in the films appearance. The amorphous films were prepared under different temperatures to the semicrystalline films, since it was assumed that the properties of the already rapid and complete curing of the amorphous films (seconds) would change very little if prepared at 100 °C.

The rapid curing process, and the FT-Raman analyses, show a rapid curing process with high consumption of both vinyl and thiol groups (Figure 3). Further detailed kinetic studies of the thiol initiation/termination steps might be interesting in order to uncover the efficiency of thiol addition using the new PPDL macromonomer, although were not run for this study since the process was found to be efficient enough for material comparison. The consumption of vinyl groups could not be determined easily from FTIR spectroscopy in the case of PPDL$_{SH}$-based films, since the polymers ester stretch at 1735 cm^{-1} obscured one of the vinyl signals at 1647 cm^{-1}. Therefore, for all films, FT-Raman spectroscopy was used to observe the loss of the vinyl bonds (i.e., 1571, 3065, and 3137 cm^{-1} for NTMP, Figure 3, and thiol groups (2568 cm^{-1})). The vinyl and thiol group absorbances were compared against the aliphatic region from before and after curing (Figure 3) to calculate the percentage

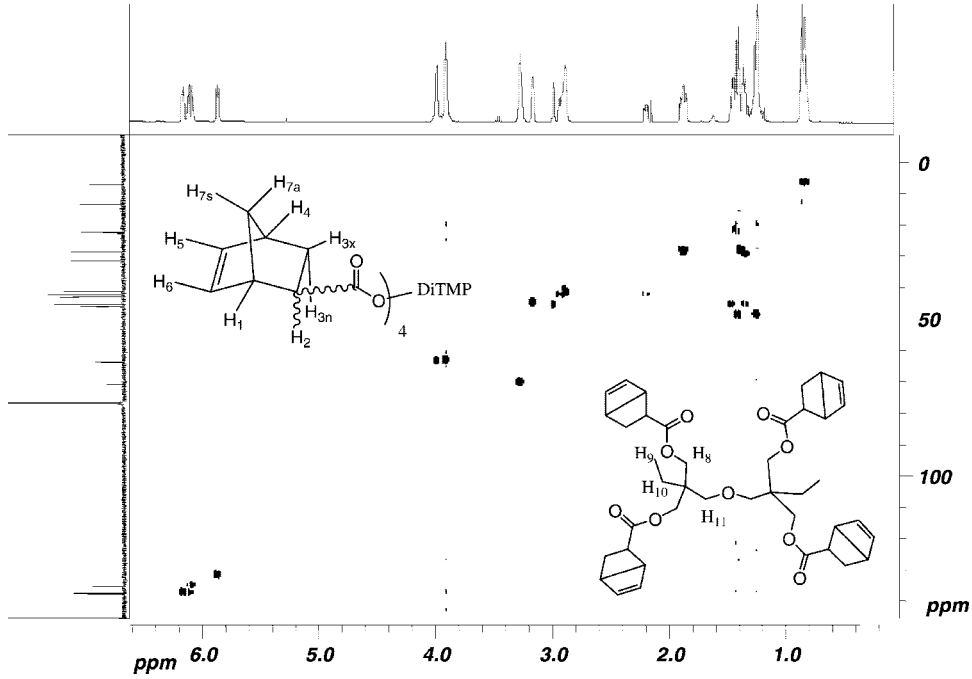

Figure 2. HMQC spectra of the tetrafunctional ene monomer, NTMP, **1**.

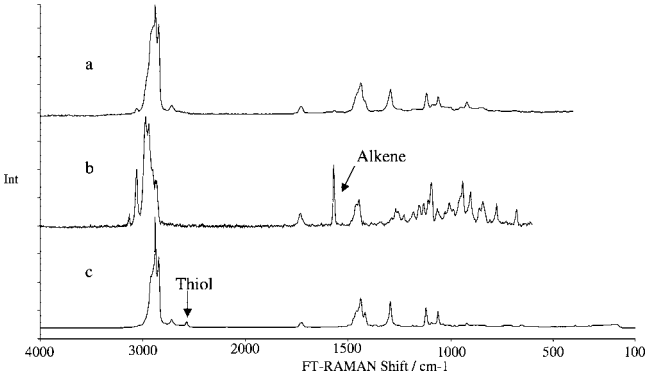

Figure 3. FT-Raman spectra: (a) NTMP−$PPDL_{SH}$ film (cured), (b) NTMP uncured, and (c) $PPDL_{SH}$ uncured.

of successful thiol−ene coupling events. Since the percent of thiol groups before curing is already small, relative to the bulk of the PPDL species, they were difficult to observe by FT-Raman spectroscopy. Therefore, we relied upon the strong vinyl signals for more reliable conversion calculations for network formation. In all cases, no residual unsaturations could be detected, suggesting that the vinyl consumption after curing was found to be essentially complete.

Thermal Analysis. The principal contributions from the different monomers examined in this work were the network density and the degree of crystallinity, both of which impact upon the final film properties. In terms of crystallinity, the DSC analysis for the monomer $PPDL_{SH}$, **3**, revealed a melting transition due to the crystalline domains at 86 °C (reported for enzyme-synthesized PPDL as 97 °C[16]) and with a melt enthalpy of 150 J g^{-1}. Pure, fully crystalline PPDL has been reported[32] to have a melting enthalpy (ΔH_m) of 233 J g^{-1}, which indicates that $PPDL_{SH}$ has a degree of crystallinity of ca. 64% (Table 1). The T_g could not be detected using DSC but has been reported to be more successfully measured (−27 °C) using relaxation techniques due to the high degree of crystallinity.[16] However, the DSC analysis did reveal a shift in melting point to lower temperatures for the cured films based on $PPDL_{SH}$ (Figure 4). The reduced crystallinity of the $PPDL_{SH}$ after curing with

Table 1. Physical Properties of Networks[a]

mixture[b]		T_g (DMA)	X_c	T_m (DSC)	ΔH_m	CA[d]	R_s[e]	strain[f]	E[g]
ene	thiol	(°C)	(%)[c]	(°C)	(J g^{-1})	(deg)	(μm)	(%)	(MPa)
1	**3**	50	43	79	100	76	1.97	53	77
1	**4**	×	−	−	−	65	−	×	×
2	**3**	46	29	71	67	75	1.26	36	47
2	**4**	15	−	−	−	57	−	38	1
none	**3**	−27	64	86	150	73	−	12	370

[a] ×, film too fragile for DMA analysis; −, not applicable. [b] See Figure 1 for molecules **1**−**4**. [c] Calculation based upon ΔH_m where 233 J g^{-1} is 100% crystalline. [d] Contact angle against water. [e] Spherulite radius taken from birefringence pattern of small-angle light scattering. [f] Calculated from DMA at yield. [g] Tensile modulus. The T_g of **3** from the literature.[16]

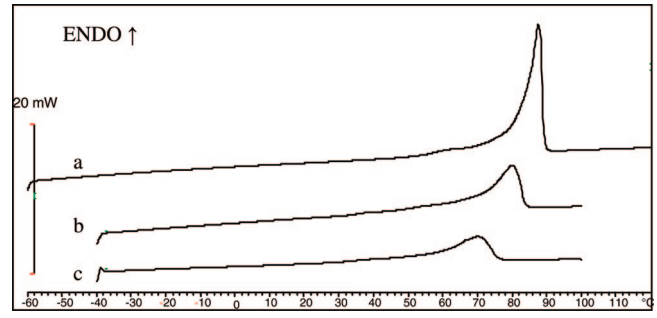

Figure 4. DSC results for (a) $PPDL_{SH}$, (b) NTMP−$PPDL_{SH}$, and (c) TMPDEA−$PPDL_{SH}$.

monomers **1** and **2** is an effect of the cross-linking. The ΔH_m of the networks decreased to 100 J g^{-1} for NTMP, **1**, and 67 J g^{-1} for TMPDEA, **2**. Both materials were fully cured as observed by FT-Raman spectroscopy, which suggests that monomer reactivity and spatial arrangement can explain the disparity. The norbornene group is known to polymerize very fast and can also homopolymerize. The higher crystallinity for the NTMP−PPDL as compared to PPDL−TMPDEA suggests that a significant amount of norbornene moieties have homopolymerized, leaving the PPDL chain segments less affected and more prone to crystallize. Subsequently, the degree of cross-linking is affected by the occurrence of homopolymerization.

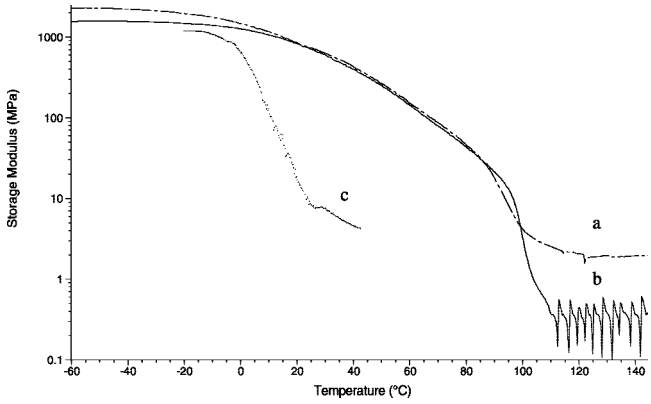

Figure 5. Storage modulus as a function of temperature for (a) TMPDEA−PPDL, (b) NTMP−PPDL, and (c) TMPDEA−TRIS.

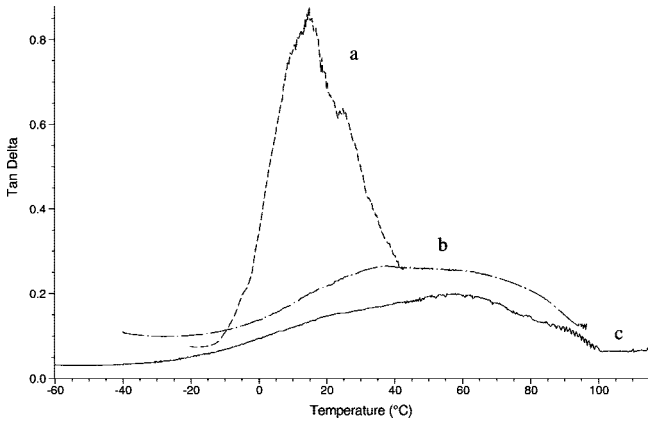

Figure 6. Tan δ as a function of temperature for (a) TMPDEA−TRIS, (b) TMPDEA−PPDL, and (c) NTMP−PPDL.

Dynamic Mechanical Analysis. The films were analyzed by dynamic mechanical thermal analysis (DMA) in order to gain more insight into mechanical properties and network structure. It was possible to obtain free-standing films for all cross-linked fims except for NTMP−TRIS, which was too fragile. Storage modulus and tan δ are shown in Figures 5 and 6. The storage modulus (Figure 5) drops significantly at ca. 10 °C for TMPDEA−TRIS which is due to the glass transition. For samples NTMP−PPDL and TMPDEA−PPDL, the modules drop gradually up to the melting transitions, 80−90 °C. It is also interesting to compare the storage modulus in the rubbery plateau region for the semicrystalline samples; the higher modulus for TMPDEA−PPDL corroborates the hypothesis the degree of cross-linking is higher than that of NTMP−PPDL.

A section of each film type (Table 1) was immersed in chloroform three times over a period of 24 h with shaking whereafter the weight loss was determined. Each film was seen to swell, indicating cross-linking, an observation in agreement with the modulus results. The TMPDEA−TRIS and TMPDEA−PPDL retained the same mass before and after the treatment. The NTMP−TRIS monomer, however, showed a reduction in mass, −17% w/w, and NTMP-PPDL, −19% w/w, which suggests that less cross-linked networks had formed, again in agreement with the lower modulus results. This indicates a small fraction of residual thiols, although not detectable in the Raman spectra.

Further information regarding the network homogeneity can be obtained from the shape of the tan δ as a function of temperature (Figure 6). The amorphous network TMPDEA−TRIS exhibits a high, rather narrow, peak indicating a homogeneous network. The semicrystalline materials, on the other hand,

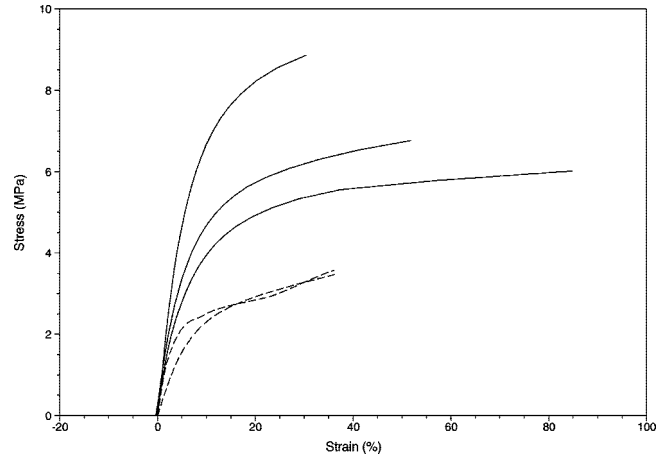

Figure 7. Repeat results for the stress−strain curves of NTMP−PPDL (line) and TMPDEA−PPDL (dashed).

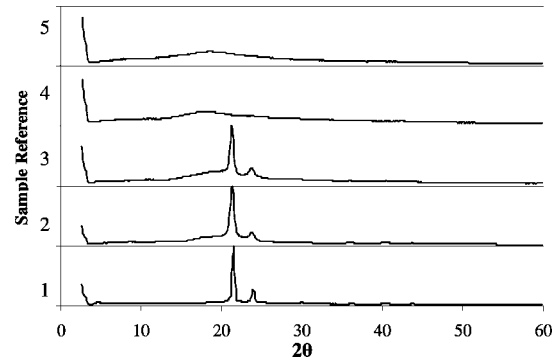

Figure 8. X-ray diffraction of polymer films: (1) $PPDL_{SH}$, (2) TMPDEA−$PPDL_{SH}$, (3) NTMP−$PPDL_{SH}$, (4) NTMP−TRIS, (5) TMPDEA−TRIS.

exhibit transitions occurring over a large temperature range from −20 to 100 °C, which suggests that the corresponding networks are rather inhomogeneous.

Tensile testing was also conducted on free-standing films using DMA (Figure 7). At room temperature all materials were too brittle to make the DMA analysis meaningful. The semicrystalline samples, TMPDEA−PPDL and NTMP−PPDL, were instead analyzed at 40 °C, above their glass transition temperatures. Several samples of each kind were analyzed, and it was difficult to obtain good reproducibility, possibly due to orientation effects from the film manufacturing. However, a number of measurements were acquired for each film to obtain average values of modulus. The measured stress and corresponding modulus of the semicrystalline materials (Figure 7) illustrate the difference in material strength based upon crystallinity. A higher modulus (77 MPa) was seen for NTMP−PPDL, despite having a lower cross-linked density than TMPDEA−PPDL, as it was a more crystalline network. As expected, TMPDEA gave a higher modulus film when part of a semicrystalline network rather than that of an amorphous network (Table 1, 44 MPa compared with 1 MPa). The modulus of the amorphous NTMP−TRIS film could not be measured since it was too fragile for such analysis.

X-ray Diffraction and Optical Microscopy. The samples were also analyzed by X-ray diffraction. The X-ray diffractograms (Figure 8) showed a similar pattern for $PPDL_{SH}$ to that of PPDL found in the literature,[33] an orthorhombic unit cell akin to PE. For example, the reflections (2θ) of PPDL−NTMP were measured at 21.4 and 23.7°, which correspond to 4.14 and 3.74 Å, respectively. Since the crystalline films gave a very similar response (i.e., Figure 8, **2** and **3**), it appeared that cross-

linking did not have an impact upon the nature of the unit cell. On the other hand, the amorphous films gave similar broad signal responses, reflecting the lack of crystallinity (Figures 8, 4, and 5). The full width at half-maximum (FWHM) in the diffractogram of the $PPDL_{SH}$ monomer was measured to be 0.3. Lower FWHM values indicate higher relative degrees of crystallinity between samples. Therefore, the increasing degree of crystallinity according to fwhm values follows: amorphous networks with TRIS (10), TMPDEA−PPDL network (0.6), NTMP−PPDL network (0.5), PPDL monomer (0.3). This order of network crystallinity supports evidence from the melting enthalpies that the NTMP monomer creates more crystalline networks than the TMPDEA monomer.

Optical microscopy was used to elucidate more concerning the crystalline nature of the samples. The broad temperature range during the glass transition is also indicative of a cross-linked crystalline system. The spherulites from the $PPDL_{SH}$ monomer were axialite in nature due to the low molecular weight and therefore the increased probability of chain entanglements. However, after cross-linking a second phase develops that can accommodate branching crystals to cover 3D space (spherulites). As a result, the crystallinity drops (as seen by the thermal and X-ray analysis), which means that the development of a superstructure is prohibited. Because of the dense cross-linked network seen for monomers **1** and **2** with $PPDL_{SH}$ and the rapid cooling after curing, small spherulites were observed (from 2 to 3 μm, Table 1), showing a clear, cloverleaf pattern from polarized light (632 nm). The spherulites impart the semitransparent nature of the films and also add other physicals properties to the film in terms of strength.

Contact Angle. The use of a hydrophobic monomer such as $PPDL_{SH}$ was expected to yield a more hydrophobic film; PE has been reported to have a contact angle of 109°.[34] As expected, the contact angles were found to be higher for the networks that used $PPDL_{SH}$ (Table 1, TMPDEA−PPDL 75° and NTMP−PPDL 76°), rather than TRIS (i.e., TMPDEA−TRIS 57° and NTMP−TRIS 65°). We attribute the lower contact angle of TMPDEA−TRIS to the acid functionality increasing hydrophilicity. However, for $PPDL_{SH}$-based films, there was never much difference in contact angle, regardless of the alkene−monomer used, which indicates that the high percent of hydrophobic $PPDL_{SH}$ monomer to alkene−monomer dictates the final hydrophibicity of the film.

Conclusion

Telechelic thiol-functionalized polypentadecalactone (PPDL) prepolymers were easily obtained by the lipase-catalyzed ring-opening of pentadecalactone using 6-mercapto-1-hexanol as initiator. γ-Thiobutyrolactone was used to afford a thiol end group once the desired chain length was obtained. The telechelic PPDL allows for the synthesis of semicrystalline networks. We have shown that thiol-functional PPDL can be readily cured utilizing ene-containing compounds, in the presence of oxygen, to create polymer networks using thiol−ene chemistry with hydrophobic character and increased modulus compared to the amorphous equivalent. The network properties were dependent upon the efficiency of thiol−ene couplings, since they had a bearing upon the crystallinity of the final network. It was surprising that networks retained crystallinity despite the restrictions imposed by the cross-linking and rapid cooling, although crystallites were small. It may be possible to tune the crystallinity to change the film properties, depending upon the reactive or steric nature of the monomer used or the manner in which the films are cooled after processing to promote spherulite growth. In addition, the TMPDEA films, both crystalline and amorphous, have free carboxylic groups that could be used for surface chemistry. The semicrystalline networks based upon PPDL may be suitable for photolithography, devices, biodegradable coatings, or even in the body as bioscaffolding.

Experimental Section

Instrumentation. ^1H and ^{13}C NMR spectra were recorded on a Bruker AM 400. Chloroform-d containing 1% (v/v) TMS was used as solvent. Size exclusion chromatography, (SEC) using chloroform (1.0 mL min^{-1}) as the mobile phase, was performed at 40 °C with a Waters 717 plus Autosampler and a Waters model 510 apparatus equipped with three Pl gel 10 μm mixed-B columns, 300 × 7.5 mm. Spectra were recorded with an Pl-ELS 1000 evaporative light scattering detector, connected to an IBM-compatible PC. Millennium software (version 3.05.01) was used to process the data. The eluent consisted of HPLC grade chloroform (95% v/v) and methanol (5% v/v). SEC samples were prepared as 0.5 mg/mL solutions using the eluent. The molecular weights were calibrated against polyester standards. Raman analysis was performed on bulk samples using Perkin-Elmer Spectrum 2000 FT-Raman. Each spectrum was based on 32 scans using 1500 mW. The MALDI-TOF-MS analysis was conducted on a Bruker UltraFlex MALDI-TOF-MS with SCOUT-MTP Ion Source (Bruker Daltonics, Bremen) equipped with a N_2 laser (337 nm), a gridless ion source, and reflector design. All spectra were acquired using a reflector-positive method with an acceleration voltage of 25 kV and a reflector voltage of 26.3 kV. Calibration was performed in order to secure good mass accuracy. As for the samples, solutions of 2−5 mM in $CHCl_3$ were each mixed with a matrix, which consisted of 0.1 M 9-nitroanthrazene dissolved in THF. The preparation protocol included mixing of 5 μL of sample with 20 μL of matrix solution. Then 1 μL of the mixture was spotted on the MALDI target and was left to crystallize at room temperature. Normally, 50 pulses were acquired for each sample. In order to achieve good mass accuracy and resolution, the analysis was performed at the laser threshold of each individual matrix/sample combination. DMA analysis was performed on a TA Instruments Q800 equipped with a film fixture for tensile testing. Film tension DMA measurements on rectangular dried film samples (20 × 6 mm) were performed between −30 and 150 °C for PPDL-based networks and −40 to 30 °C from TRIS-based networks, with a heating rate of 2 °C/min for all analyses. The tests were performed in controlled strain mode with a frequency of 1 Hz, oscillating amplitude of 45 μm, and force track of 130%. The stress/strain measurements were measured at 3 N/min and at 40 °C for PPDL-based networks and at 25−40 °C for TRIS-based networks. Spherulite measurements were made by passing a He−Ne 632 nm laser through the film and polarizers (131° horizontal and 230° vertical) and measuring the projected pattern. A Marwell M1805, class 3b, 6 mW laser source was used. Calculations of spherulite size were made using the Stein equation from the various angle and distance measurements obtained for each pattern. Powder diffractograms were obtained at room temperature between scattering angles, 2θ, of 5−60° using a Philips XÇPert-MPD diffractometer, giving a clear identification of the different crystal modifications; no features were seen between 60 and 90°. Monochromatic Cu Kα radiation was employed. Differential scanning calorimetry (DSC) thermograms were collected using a Mettler Toledo DSC820 using a heating/cooling rate of 10 °C min^{-1} under a nitrogen atmosphere. STAR^e software (version 8.10) was used to evaluate data.

Materials. Trimethylolpropane diallyl ether (TMPDE) was supplied by Perstorp AB, Sweden, and purified using a silica column. TMPDE eluted at 5:95 (EtOAc:heptane), with an R_f = 0.7 in 50:50 (EtOAc:heptane). 5-Norbornene-2-carboxylic acid, mixture of *exo* and *endo* isomers (Sigma, 98%), 4-(dimethylamino)pyridine (Acros, 99%), pyridine (VWR, 99.7%), and *N,N′*-dicyclohexylcarbodiimide (DCC, Acros, 99%) were all used as received, Novozyme 435 was purchased from Aldrich, dried under vacuum, and stored over P_2O_5 before use. 6-Mercapto-1-hexanol was obtained from Fluka. PDL (Sigma) was dried under vacuum 24 h before the reaction. Trimethylolpropane tris(2-mercaptoacetate) (TRIS) was supplied by Bruno Boch, Germany.

TMPDEA, 2. TMPDE (18.5 g, 86 mmol), maleic anhydride (20.2 g, 205 mmol), PTSA (0.6 g), toluene (200 mL), and a catalytic amount of hydroquinone were left overnight at 80 °C under stirring. The product was filtered to remove solids, then quenched overnight with the addition of 50 mL of water and 5 mL of THF, and then extracted with toluene and water. The product was dried and purified by column chromatography. The product eluted at 15/85 EtOAc/heptane plus 1% acetic acid. TLC (silica) 50:50 (EtOAc:heptane plus 1% acetic acid), $R_f = 0.5$. Pure TMPDEA was obtained as a pale yellow oil (17 g, 63% yield). δ ^{1}H NMR ($CDCl_3$): δ 0.80 (t, 3H, $-CH_2CH_3$), 1.37 (q, 2H, $-CH_2CH_3$), 3.27 (s, 4H, $OCH_2CH=$), 3.90 (dt, 4H, $-CCH_2OCH_2-$, J = 5.2 Hz), 4.00 (s, 2H, $-CHCO_2CCH_2C-$), 5.15 (m, 4H, $-CH=CH_2$, J = 58 Hz), 5.83 (m, 2H, $-CH=CH_2$, J = 38 Hz), 6.35 (dd, 2H, $-CO_2CH=CHCO_2H$). ^{13}C NMR ($CDCl_3$): δ 7.4 (CH_3CH_2C-), 22.5 (CH_3CH_2C-), 41.8 (tertiary carbon $-C(CH_2)_4-$), 65.0 ($-OCH_2C(CH_2)_4-$), 70.0 ($-CCH_2OCH_2CH=$), 71.3 ($-CCH_2O-CH_2CH=$), 116.0 ($-OCH_2CH=CH$), 127.8 ($HO_2CH=CHCO_2-CH_2-$), 131.8 ($HO_2CH=CHCO_2CH_2-$), 135.1 ($-OCH_2CH=CH_2$), 165.0 ($HO_2CH=CHCO_2CH_2-$), 166.4 ($HO_2CH=CHCO_2CH_2-$). FTIR (cm^{-1}): 2967 br (OH carboxylic acid and CH_3), 2864 (CH_2), 1730 s (C=O ester), 1708 s (C=O ester), 1645 (C=C), 1460 (CH_2), 1416 (C−O), 1210 (C−O), 1163 (C−O), 1088, 993 (C−H vinyl), 921 (C−H vinyl), 852, 819, 781. FT-Raman: 3047 (CH_2 vinyl), 3008 (CH_2 vinyl), 2935 (CH_3), 2875 (CH_2), 1731 (C=O), 1641 (C=C), 1449 (CH_2), 1286 (CO−O), 998 (C=C trans), 900 (C=C cis), 769.

Norbornene Anhydride. 5-Norbornene-2-carboxylic acid (50 g, 0.36 mol), DCC (37 g, 0.18 mol), and 90 mL of dichloromethane were left with stir, at room temperature, for 24 h. The mixture was then filtered to remove the *N*-acylurea byproduct and then reduced in solvent. The norbornene anhydride was precipitated from dichloromethane into *n*-hexane and then isolated by filtration to give a pure product (40 g, 80% yield). δ ^{1}H NMR ($CDCl_3$): δ 1.30 (m, 6H, H_{7a}-*endo*), 1.47 (m, 15H, H_{7a}-*exo* H_{7s}-endo H_3-*endo*), 1.93 (m, 7H, H_3-*exo*), 2.30 (m, 1H, H_2-*exo*), 2.90 (s, 5H, H_4-*endo*), 3.00 (m, 4H, H_2-*endo*), 3.15 (s, 1H, H_1-*exo*), 3.24 (s, 4H, H_1-*endo*), 6.00 (m, 4H, H_6-*endo*), 6.14 (m, 2H, H_6 and H_5 *exo*), 6.23 (m, 4H, H_5-*endo*). ^{13}C NMR ($CDCl_3$): δ 28.8 (C3-*endo*), 30.0 (C3-*exo*), 41.5 (C4-*exo*), 42.4 (C4-*endo*), 44.2 (C2-*exo*), 44.5 (C2-*endo*), 45.7 (C1-*endo*), 46 (C1-*exo*), 46.2 (C7-*exo*), 49.5 (C7-*endo*), 131.7 (C6-*endo*), 135.2 (C6-*exo*), 138.1 (C5-*endo*), 138.3 (C5-*exo*), 170.3 (C8-*endo*), 171.9 (C8-*exo*).

NTMP Monomer Synthesis. DiTMP (6.45 g, 26 mmol) and DMAP (0.6 g, 4.9 mmol) were dissolved in pyridine (40 g, 500 mmol) and 50 mL of DCM. Norbornene anhydride (40 g, 155 mmol) was dissolved in 100 mL of DCM and then added to the reaction. The mixture was left to stir at room temperature overnight until the anhydride had completely reacted (as seen by ^{13}C NMR). The reaction was then diluted with a further 50 mL of DCM, 10 mL of water, and 2 mL of THF and left to stir overnight to quench the excess anhydride. The product was diluted with a further 50 mL of DCM and washed four times with $NaHSO_4$ (10% w/v) and $NaHCO_3$ (10% w/v) and once with water. The DCM was then removed and the mixture purified using column chromatography, moving slowly from 5 to 9% diethyl ether in heptane. The product was isolated as a clear liquid, 17.2 g (91% yield). TLC (silica) 50:50 EtOAc:heptane $R_f = 0.75$. δ ^{1}H NMR ($CDCl_3$): δ 0.85 (m, 8H, H_9), 1.24 (m, 7H, H_{7a}-*endo*), 1.40 (m, 11H, H_{7a}-*exo* H_{7s}-*endo* H_3-*endo*H_{10}), 1.88 (m, 3H, H_3-*exo*), 2.20 (m, 1H, H_2-*exo*), 2.9 (m, 5H, H_4-*endo* H_2-*endo*), 3.00 (s, 1H, H_1-*exo*), 3.17 (s, 2H, H_1-*endo*), 3.28 (m, 3H, H_{11}), 3.91 (m, 4H, H_8), 3.99 (m, 3H, H_8), 5.87 (m, 2H, H_6-*endo*), 6.10 (m, 2H, H_6 and H_5 *exo*), 6.17 (m, 2H, H_5-*endo*). ^{13}C NMR ($CDCl_3$): δ 7.14 (*C*H3- of diTMP), 13.78, 22.34 (CH_3CH_2- of diTMP), 28.8 (C3-*endo*), 30.0 (C3-*exo*), 41.3 (C4-*exo*), 41.4 (C4-*endo*), 42.1 (C2-*exo*), 42.8, 43.0 (*tert*-C of diTMP) 45.4 (C2-*endo*), 46.1 (C1-*endo*), 46.2 (C1-*exo*), 49.3 (C7-*endo*), 63.7 (two signals, $-CO_2-CH_2-C-$ of diTMP), 70.8 ($-C-CH_2-O-CH_2-C-$ of diTMP), 131.9 (C6-*endo*), 135.32 (C6-*exo*), 137.5 (C5-*endo*), 137.7 (C5-*exo*), 174.0 (C8-*endo*), 175.5 (C8-*exo*). FTIR (cm^{-1}): FT-Raman (cm^{-1}): 3137 w (CH_2 vinyl), 3065 m (CH_2 vinyl), 2972 (CH_3), 2940 (CH_2), 1729 (C=O), 1571 (C=C), 1447 (CH_2), 1269, 1104 (C−O), 941 (C=C def), 902 (C=C def), 851 (C−O), 773. MALDI-TOF-MS signals at (*m*/*z*) 696 (18%), 753 (74%), 889 (8%).

Poly-PDL with Two Thiol Ends (3). 6-Mercapto-1-hexanol (110 μL, 0.83 mmol) and ω-pentadecalactone (1 g, 4.15 mmol) were mixed in a 15 mL round reaction flask. Addition of 40 mg of Novozyme 435 started the reaction that was allowed to run for 20 h. Then, γ-thiobutyrolactone (1.72 mL, 20.75 mmol) was added, and the reaction was allowed to run for 24 h. ^{1}H NMR (400 MHz, $CDCl_3$, δ in ppm): 4.05 (2H, t, CH_2CH_2OCO-), 2.57 (2H, q, $-CH_2CH_2SH$), 2.52 (2H, q, $HSCH_2CH_2-$), 2.45 (2H, t, $-C(O)CH_2CH_2CH_2SH$), 2.28 (2H, t, $-OC(O)CH_2CH_2-$), 1.94 (2H, p, $-CH_2CH_2CH_2SH$), 1.61−1.69 (4H, m, $-CH_2CH_2(CH_2)_{10}-CH_2CH_2-$), 1.18−1.39 (20H, m, $-CH_2CH_2(CH_2)_{10}CH_2CH_2-$). ^{13}C NMR (400 MHz, $CDCl_3$, δ in ppm): 173.9 (C=O, C-1), 34.4 ($COCH_2CH_2$), 25.4 ($SHCH_2CH_2CH_2$-, initiator), 33.8 ($SHCH_2C-H_2CH_2-$, initiator), 64.1 ($HS(CH_2)_5CH_2O-$, initiator), 64.4 ($-CH_2O-$), 32.7 ($-CH_2CH_2CH_2SH$, terminator), 29.1 ($-CH_2CH_2-CH_2SH$, terminator), 24 ($-CH_2CH_2CH_2SH$, terminator).

General Procedure for TMPDEA−TRIS Photopolymerization. A vial was charged with TMPDEA (2 g, 6.4 mmol), initiator I-651 (40 mg, as 1% w/w), TRIS (2.28 g, 5.7 mmol), and Texanol (15 mg) and mixed until homogeneous. The solution was then applied as a film, using a 90 μm applicator, to a glass substrate cured by five successive passes of the film under a Fusion system model 300 UV lamp (H bulb), giving a total dose of 500 mJ/cm^2, and then left to cool. A smooth, transparent film was produced. FTIR (cm^{-1}): 2967 br (OH carboxylic acid and CH_3), 2864 (CH_2), 1730 s (C=O ester), 1460 (CH_2), 1416 (C−O), 1210 (C−O), 1163 (C−O), 1088, 993 (C−H vinyl), 921 (C−H vinyl), 852, 819, 781. FT-Raman: 3047 (CH_2 vinyl), 3008 (CH_2 vinyl), 2935 (CH_3), 2875 (CH_2), 2546 (−SH, present if unreacted), 1731 (C=O), 1641 (C=C, present if unreacted), 1449 (CH_2), 1286 (CO−O), 998 (C=C trans), 900 (C=C cis), 769.

General Procedure for TMPDEA−PPDL Photopolymerization. A vial was charged with TMPDEA (0.5 g, 1.6 mmol), initiator I-651 (20 mg, as 1% w/w), $PPDL_{SH}$ (1.48 g, 1.1 mmol), and Texanol (15 mg, 1% w/w) and left at 100 °C for 15 min. The solution was then applied as a film, using a heated 90 μm applicator, to a glass substrate cured in the molten state by five successive passes of the film under a Fusion system model 300 UV lamp (H bulb), giving a total dose of 500 mJ/cm^2, and then left to cool and recrystallize. A smooth, transparent film was produced which cooled and recrystallized to give a slightly opaque film. FTIR (cm^{-1}): 2967 br (OH carboxylic acid and CH_3), 2864 (CH_2), 1730 s (C=O ester), 1460 (CH_2), 1416 (C−O), 1210 (C−O), 1152 (C−O), 990, 778. FT-Raman: 3047 (CH_2 vinyl), 3008 (CH_2 vinyl), 2935 (CH_3), 2875 (CH_2), 2709, 2562 (−SH, present if unreacted), 1731 (C=O), 1641 (C=C, present if unreacted), 1449 (CH_2), 1286 (CO−O), 733, 652.

General Procedure for NTMP−TRIS Photopolymerization. A vial was charged with NTMP (0.5 g, 0.67 mmol), initiator I-651 (10 mg, as 1% w/w), TRIS (0.52 g, 1.3 mmol), and Texanol (15 mg) and mixed until homogeneous. The solution was then applied as a film, using a 90 μm applicator, to a glass substrate cured by five successive passes of the film under a Fusion system model 300 UV lamp (H bulb), giving a total dose of 500 mJ/cm^2, and then left to cool. A smooth, hard transparent film was produced. FTIR (cm^{-1}): 2917 s (CH_3), 2850 s (CH_2), 1728 (C=O), 1571 (C=C, present if unreacted), 1463 (CH_2), 1269, 1104 (C−O), 941 (C=C def), 902 (C=C def), 851 (C−O), 773. FT-Raman (cm^{-1}): 2880 (CH_3), 2847 (CH_2) 2546 (−SH, present if unreacted), 1723 (C=O), 1571 (C=C, present if unreacted), 1435 (CH_2), 1293, 1118 (C−O), 919.

General Procedure for NTMP−PPDL Photopolymerization. A vial was charged with NTMP (0.2 g, 0.27 mmol), initiator I-651 (9 mg, as 1% w/w), $PPDL_{SH}$ (0.73 g, 0.52 mmol), and Texanol (15 mg) and left at 80 °C until a melt was seen. The solution was then applied as a film, using a heated 90 μm applicator, to a glass substrate cured in the molten state by five successive passes of the film under a Fusion system model 300 UV lamp (H bulb), giving

a total dose of 500 mJ/cm^2, and then left to cool and recrystallize. A smooth, transparent film was produced which cooled and recrystallized to give a slightly opaque film. FTIR (cm^{-1}): 2917 s (CH_3), 2850 s (CH_2), 1728 (C═O), 1571 (C═C, present if unreacted), 1463 (CH_2), 1269, 1104 (C−O), 941 (C═C def), 902 (C═C def), 851 (C−O), 773. FT-Raman (cm^{-1}): 2880 (CH_3), 2847 (CH_2), 2709, 2562 (−SH, present if unreacted), 1723 (C═O), 1571 (C═C, present if unreacted), 1436 (CH_2), 1293, 1118 (C−O), 919.

Acknowledgment. The research has been supported by a Marie Curie Action RTN Biocatalytic Approach to Material Design BIOMADE (Contract No. MRTN-CT-2004-505147). We thank Prof. Ulf Gedde and Dr. George Vamvounis for their helpful discussions regarding the crystallinity and X-ray analysis.

References and Notes

(1) Hoyle, C. E.; Lee, T. Y.; Roper, T. *J. Polym. Sci., Part A: Polym. Chem.* **2004**, *42*, 5301–5338.
(2) Jacobine, A. F. In *Radiation Curing in Polymer Science*; Fouassier, J. P., Rabek, J. F., Eds.; Elsevier: London, 1993, pp 219−264.
(3) Lu, H.; Carioscia, J. A.; Stansbury, J. W.; Bowman, C. N. *Dent. Mater.* **2005**, *21*, 1129–1136.
(4) Cramer, N. B.; Reddy, S. K.; Lu, H.; Cross, T.; Raj, R.; Bowman, C. N. *J. Polym. Sci., Part A: Polym. Chem.* **2004**, *42*, 1752–1757.
(5) Harant, A. W.; Khire, V. S.; Thibdaux, M. S.; Bowman, C. N. *Macromolecules* **2006**, *39*, 1461–1466.
(6) Khire, U. S.; Harant, A. W.; Watkins, A. W.; Anseth, K. S.; Bowman, C. N. *Macromolecules* **2006**, *39*, 5081–5086.
(7) Boileau, S.; Mazeaud-Henri, B.; Blackborow, R. *Eur. Polym. J.* **2003**, *39*, 1395–1404.
(8) Metters, A. T.; Anseth, K. S.; Bowman, C. N. *J. Phys. Chem. B* **2001**, *105*, 8069–8076.
(9) Takwa, M.; Simpson, N. J.; Malmström, E.; Hult, K.; Martinelle, M. *Macromol. Rapid Commun.* **2006**, *27*, 1932–1936.
(10) Bisht, K. S.; Henderson, L. A.; Gross, R. A.; Kaplan, D. L.; Swift, G. *Macromolecules* **1997**, *30*, 2705–2711.
(11) Kobayashi, S.; Uyama, H.; Namekawa, S. *Polym. Degrad. Stab.* **1998**, *59*, 195–201.
(12) Noda, S.; Kamiya, N.; Goto, M.; Nakashio, F. *Biotechnol. Lett.* **1997**, *19*, 307–309.
(13) Kalra, B.; Kumar, A.; Gross, R. A. *Macromolecules* **2004**, *37*, 1243–1250.
(14) Focarete, M. L.; Gazzano, M.; Scandola, M. *Macromolecules* **2002**, *35*, 8066–8071.
(15) Ceccorulli, G.; Scandola, M. *Biomacromolecules* **2005**, *6*, 902–907.
(16) Focarete, M. L.; Scandola, M.; Kumar, A.; Gross, R. A. *J. Polym. Sci., Part B: Polym. Phys.* **2001**, *39*, 1721–1729.
(17) Yamane, H.; Teraoa, K. S.; Hikib, Y. K.; Kimurab, Y.; Saitoc, T. *Polymer* **2001**, *42*, 78773–7878.
(18) Sinha, V. R.; Bansal, K.; Kaushik, R.; Kumria, R.; Trehan, A. *Int. J. Pharm.* **2004**, *278*, 1–23.
(19) Odian, G. *Principles of Polymerization*; Wiley-Interscience: New York, 1991.
(20) Bixler, H. J.; Sweeting, O. J. In *The Science and Technology of Polymer Films*; Sweeting, O. J., Ed.; John Wiley & Sons: New York, 1971; Vol. *2*.
(21) Lagerwall, J. P. F.; Giesselmann, F. *Chem. Phys. Chem.* **2006**, *7*, 20–45.
(22) Xie, P.; Zhan, R. *J. Mater. Chem.* **2005**, *15*, 2529–2550.
(23) Zhu, G.; Liang, G.; Xu, Q.; Yu, Q. *J. Appl. Polym. Sci.* **2003**, *90*, 1589–1595.
(24) Claesson, H.; Scheurer, C.; Malmström, E.; johansson, M.; Hult, A.; Paulus, W.; Schwalm, R. *Prog. Org. Coat.* **2004**, *49*, 13–22.
(25) Nùñez, E.; Ferrando, C.; Malmström, E.; Claesson, H.; Werner, P.-E.; Gedde, U. W. *Polymer* **2004**, *45*, 5251–5263.
(26) Simon, D.; Holland, A.; Shanks, R. *J. Appl. Polym. Sci.* **2007**, *103*, 1287–1294.
(27) Ahn, S.-H.; An, J. A.; Lee, D. S.; S. C K. *J. Polym. Sci., Part B: Polym. Phys.* **2003**, *31*, 1627–1639.
(28) Kyristsis, K.; Pissis, P.; Grigorieva, O. P.; Sergeeva, L. M.; Brouko, A. A.; Zimich, O. N.; Privalko, E. G.; Shtompel, V. I.; Privalko, V. P. *J. Appl. Polym. Sci.* **1999**, *73*, 385–387.
(29) Du, P.; Xu, Q.; Xue, Y.; Ngo, S.; Okuda, J.; Frish, H. L. *Macromolecules* **1994**, *27*, 2757–2760.
(30) Orhum, M., Ebru, O. US, Vol. WO2005074619, **2005**.
(31) Abd-El-Aziz, A. S.; May, L. J.; Edel, A. L. *Macromol. Rapid Commun.* **2000**, *21*, 598–602.
(32) Lebedev, B.; Yevstropov, A. *Makromol. Chem.* **1984**, *185*, 1235.
(33) Gazzano, M.; Malta, V.; Focarete, M. L.; Scandola, M.; Gross, R. A. *J. Polym. Sci., Part B: Polym. Phys.* **2003**, *41*, 1009–1013.
(34) Sweeting, O. J. In *The Science and Technology of Polymer Films*; Sweeting, O. J., Ed.; John Wiley & Sons: New York, 1971; Vol. *2*.

MA702419M